Supplementary information

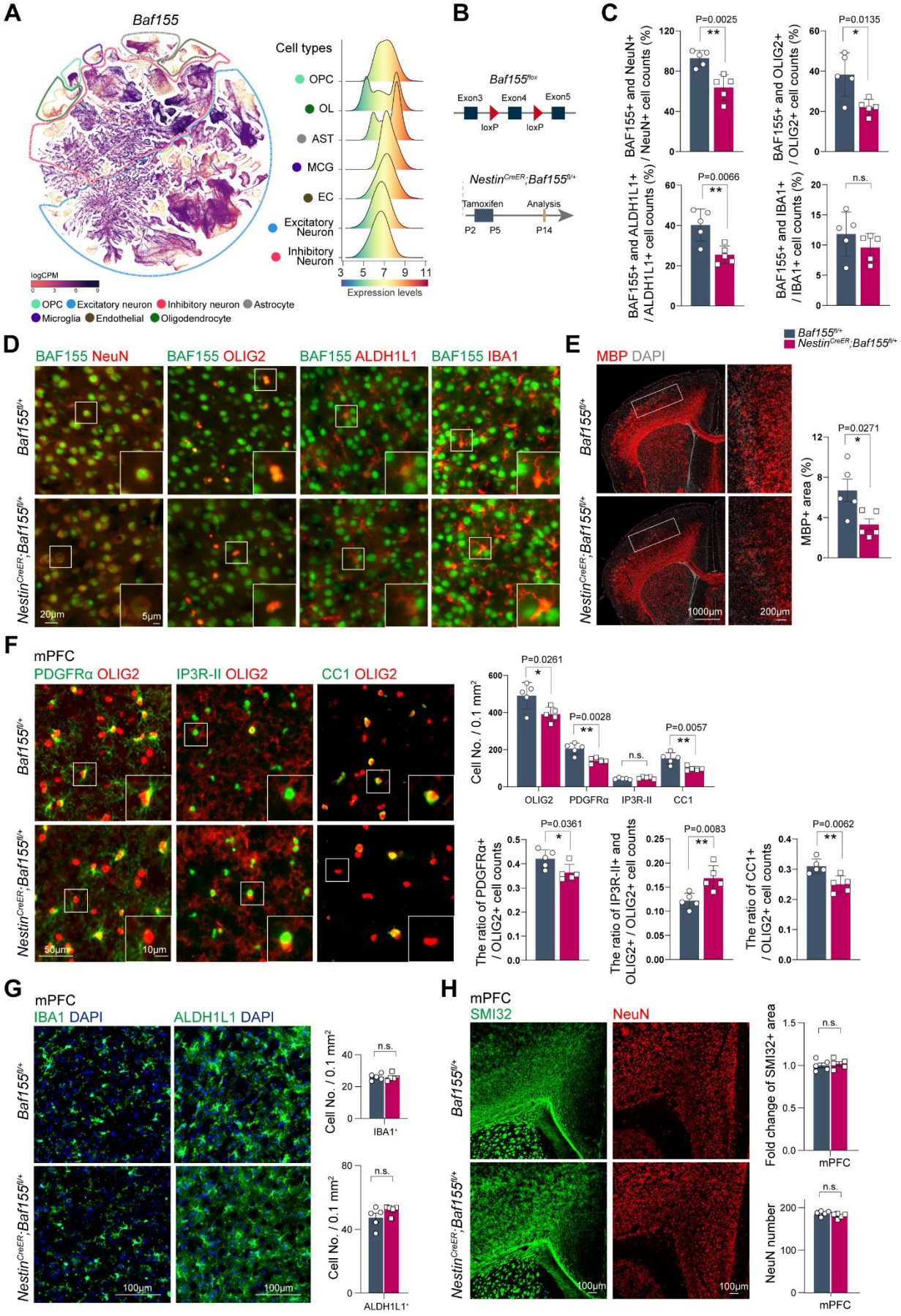

Supplementary Figure 1. Loss of BAF155 in neural stem cells induces hypomyelination

(A) UMAP plot shown the *Baf155* gene expression in different cell type of whole mouse brain from mouse whole-brain transcriptomic cell type atlas of The Allen Brain Cell Atlas.

(B) Establishment of $Nestin^{CreERT2};Baf155^{fl/+}$ mouse strain and the experimental diagram.

(C, D) Representative images of co-staining of BAF155 with cell type markers: NeuN, Aldh1L1, OLIG2, IBA1 for brain cells in $Nestin^{CreERT2};Baf155^{fl/+}$ mice. The quantification shows the reduced BAF155 protein levels in neural stem-cell-derived neurons, astrocytes, and oligodendroglia, but not in microglia, n = 5 mice.

(E) Representative images of MBP staining and quantification of MBP+ area. Scale bar = 1000 μm and 200 μm, n = 5 mice.

(F) Representative images and quantifications of co-staining for PDGFRα/OLIG2, IP3R-II/OLIG2 and CC1/OLIG2 in the mPFC of $Nestin^{CreERT2};Baf155^{fl/+}$ mice. Scale bar = 50 μm and 10 μm, n = 5 mice.

(G) Representative images and quantifications of IBA1, and ALDH1L1 staining in mPFC. Scale bar = 100 μm, n = 5 mice.

(H) Representative images of SMI32 labeling of neural filament in mPFC and quantification of SMI32+ area in mPFC. Scale bar = 100 μm, n = 5 mice. Representative images in NeuN staining in mPFC and quantification of NeuN+ cell numbers. Scale bar = 100 μm, n = 5 mice.

The significance between the two experimental groups was ascertained using the unpaired t-test. All statistical tests were two-tailed. Data presented as mean ± SEM; n.s. not significant, *$p < 0.05$, **$p < 0.01$, ***$p < 0.001$, ****$p < 0.0001$.

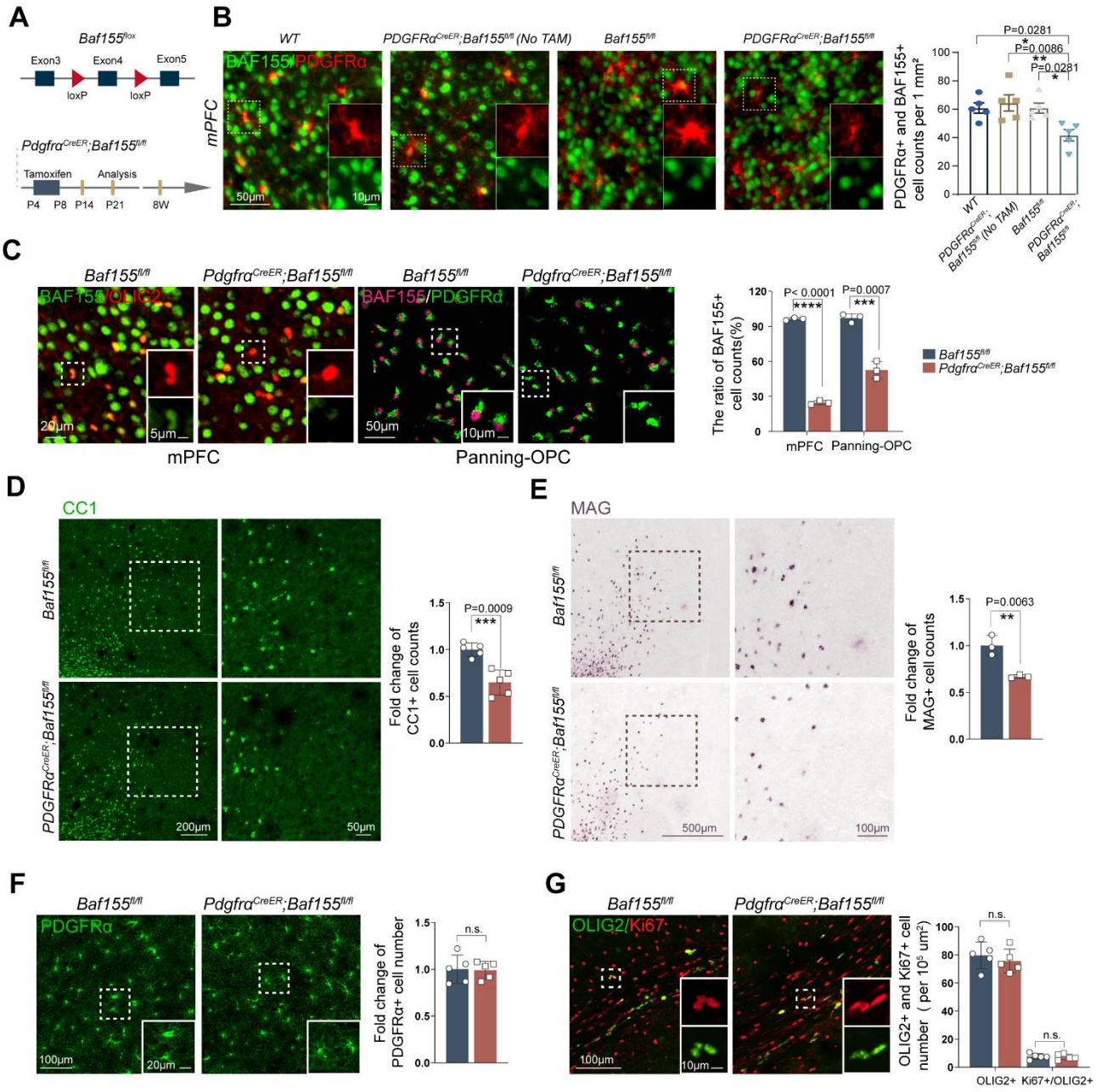

Supplementary Figure 2. BAF155 regulates oligodendroglial differentiation and myelination

(A) Establishment of *Pdgfrα*^{CreER}*;Baf155*$^{fl/fl}$ mouse strain and the experimental diagram.

(B) Representative images and quantifications of co-staining of BAF155 and PDGFRα in four mouse groups (WT without tamoxifen vs. *Baf155*$^{fl/fl}$ without tamoxifen vs. *Pdgfrα*^{CreER}*;Baf155*$^{fl/fl}$ without tamoxifen vs. *Pdgfrα*^{CreER}*;Baf155*$^{fl/fl}$ with tamoxifen). Scale bar = 50 μm and 10 μm, n = 5 mice.

.

(C) Verification of knockout efficiency in *Pdgfrα*^{CreER};*Baf155*$^{fl/fl}$ mouse both *in vivo* (Scale bar = 20 μm and 5 μm, n = 3 mice) and *in vitro* (Scale bar = 50 μm and 10 μm, n = 3 biological replicates).

(D) Representative images of CC1 staining in the mPFC of *Pdgfrα*^{CreER};*Baf155*$^{fl/fl}$ and control mice at P14 and the number of CC1+ cells in this region. Scale bar = 200 μm and 50 μm, n = 5 mice.

(E) In situ hybridization images of MAG expression in the mPFC from *Pdgfrα*^{CreER};*Baf155*$^{fl/fl}$ and control mice at P14 and the number of MAG+ cells in this region. Scale bar = 500 μm and 100 μm, n = 3 mice.

(F) Representative images of PDGFRα staining in the mPFC of *Pdgfrα*^{CreER};*Baf155*$^{fl/fl}$ and control mice at P14 and the number of PDGFRα+ cells in this region. Scale bar = 100 μm and 20 μm, n = 5 mice.

(G) Representative images of OLIG2 and Ki67 staining in *Pdgfrα*^{CreER};*Baf155*$^{fl/fl}$ and control mice at P14 and the number of OLIG2+ and OLIG2+/Ki67+ cells. Scale bar = 100 μm and 10 μm, n = 5 mice.

The significance between the two experimental groups was ascertained using the unpaired t-test. All statistical tests were two-tailed. Data presented as mean ± SEM; n.s. not significant, *p < 0.05, **p < 0.01, ***p < 0.001, ****p < 0.0001.

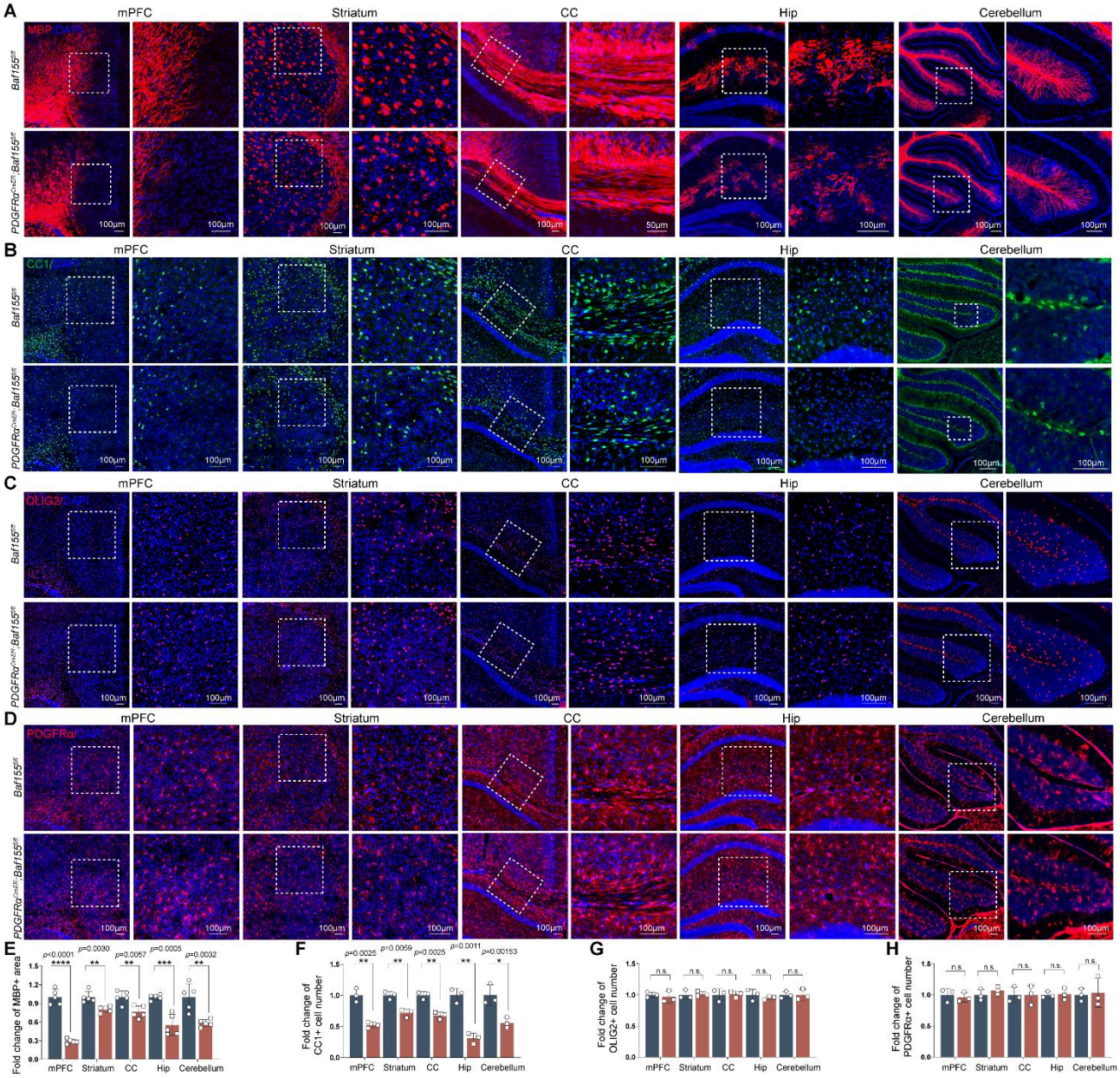

Supplementary Figure 3. Loss of BAF155 impairs OPC differentiation and myelination in development

(A-D) Representative low magnification images of MBP, CC1, OLIG2, PDGFR*α* staining of different brain regions, alongside the results shown in Figure 3A. Scale bar = 100 μm.

(E-H) Quantifications of MBP, CC1, OLIG2, PDGFR*α* staining of different brain regions, alongside the results shown in Figure 3A. n=5 mice in MBP staining; n=3 mice in CC1, OLIG2 and PDGFR*α*

staining.

The significance between the two experimental groups was ascertained using the unpaired t-test. All statistical tests were two-tailed. Data presented as mean ± SEM; n.s. not significant, *$p < 0.05$, **$p < 0.01$, ***$p < 0.001$, ****$p < 0.0001$.

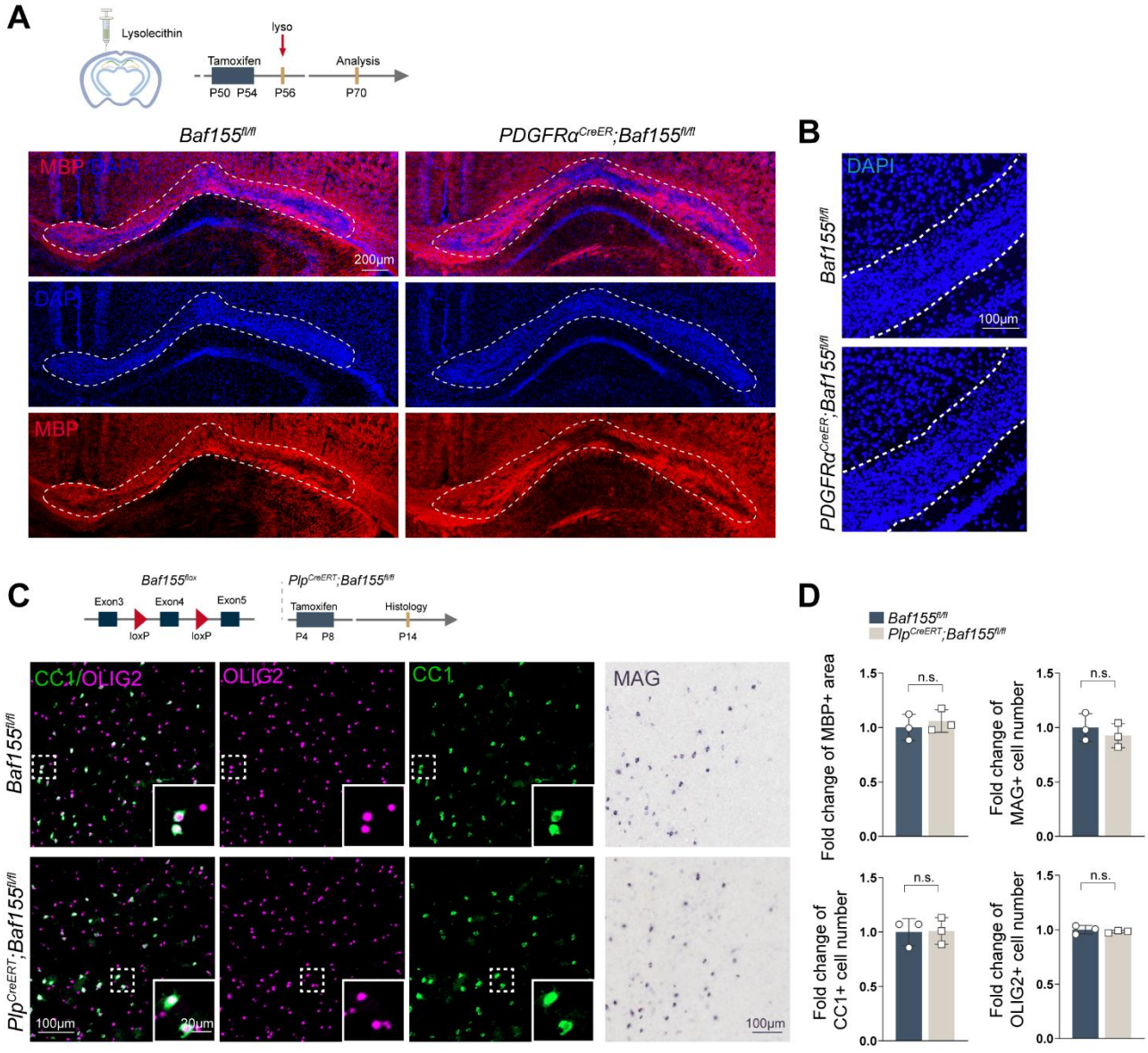

Supplementary Figure 4. Loss of BAF155 impairs OPC differentiation and remyelination

(A) Representative images of MBP staining to define the lesion areas in the corpus callosum of *Pdgfrα*^{CreER}*; Baf155*$^{fl/fl}$ and control mice at 14 days post-lesion. Scale bar = 200 μm.

(B) Representative images of DAPI staining to define the lesion areas of *Pdgfrα*^{CreER}*; Baf155*$^{fl/fl}$ and control mice, alongside the MAG in situ hybridization shown in Figure 3B. Scale bar = 100 μm.

(C, D) Representative images and quantifications of CC1/OLIG2 co-staining, and MAG in situ hybridization in *Plp*^{CreERT}*;Baf155*$^{fl/fl}$ and control mice at P14. Scale bar = 100 μm and 20 μm, n=3

mice.

The significance between the two experimental groups was ascertained using the unpaired t-test. All statistical tests were two-tailed. Data presented as mean ± SEM; n.s. not significant.

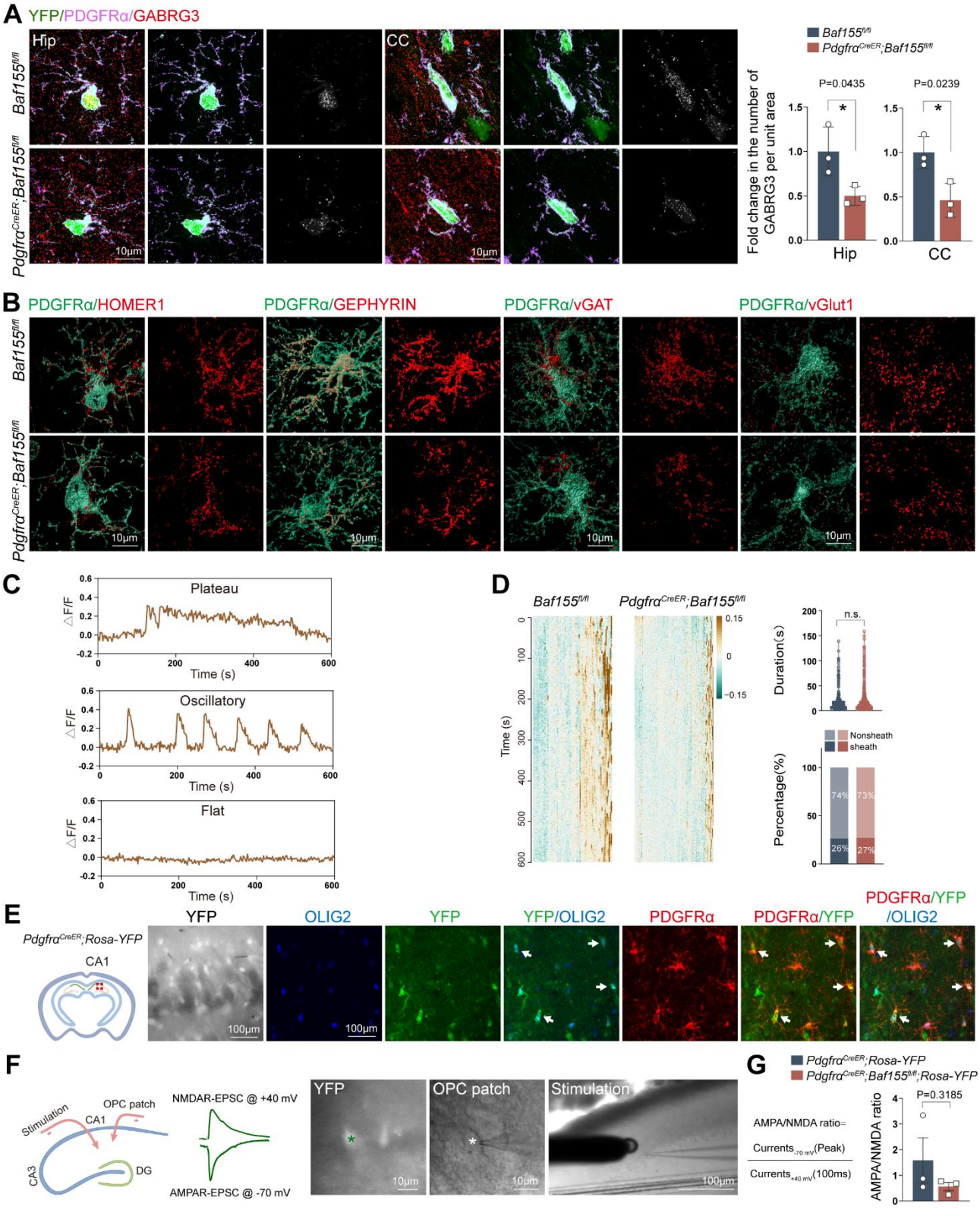

Supplementary Figure 5. BAF155 regulates OPC-neuron synaptic connection

(A) Representative images of YFP, PDGFRα and GABRG3 staining in the hippocampus and corpus

callosum of *Pdgfrα^{CreER}; Baf155$^{fl/fl}$; Rosa-YFP* and control mice at P14. The number of GABRG3 per unit of PDGFRα+ area. Scale bar = 10 μm, n=3 mice.

(B) Surface rendering image of immunofluorescence staining of PDGFRα/HOMER1, PDGFRα/Gephyrin, PDGFRα/vGAT, PDGFRα/vGLUT1 in the mPFC of *Pdgfrα^{CreER};Baf155$^{fl/fl}$* and control mice at P14, alongside the results shown in Figure 5C. Scale bar = 10 μm.

(C) Representative recordings of type 1~3 calcium waves.

(D) Representative calcium wave recording of OPC in brain slices. Right: quantification of calcium wave duration of each cell and the percentage of nonsheath or sheath forming oligodendroglia.

(E) Representative images of YFP, PDGFRα and OLIG2 staining in the hippocampus CA1 region of *Pdgfrα^{CreER}; Rosa-YFP* mice. Scale bar = 100 μm.

(F) Schematic cartoon indicates the experimental workflows of electrophysiological whole-cell recording for AMPAR and NMDAR-mediated eEPSCs from YFP^{+} OPCs in the CA1 region. Scale bar = 10 μm and 100 μm.

(G) Left panel: the formula for calculating the AMPA/NMDA ratio. Right panel: bar graphs, overlaid with the actual data points, show the AMPA/NMDA ratios for *Pdgfrα^{CreER};Rosa-YFP* and *Pdgfrα^{CreER};Baf155$^{fl/fl}$;Rosa-YFP* OPCs, n= 3 OPCs.

The significance between the two experimental groups was ascertained using the unpaired t-test. All statistical tests were two-tailed. Data presented as mean ± SEM; n.s. not significant, *$p < 0.05$, **$p < 0.01$.

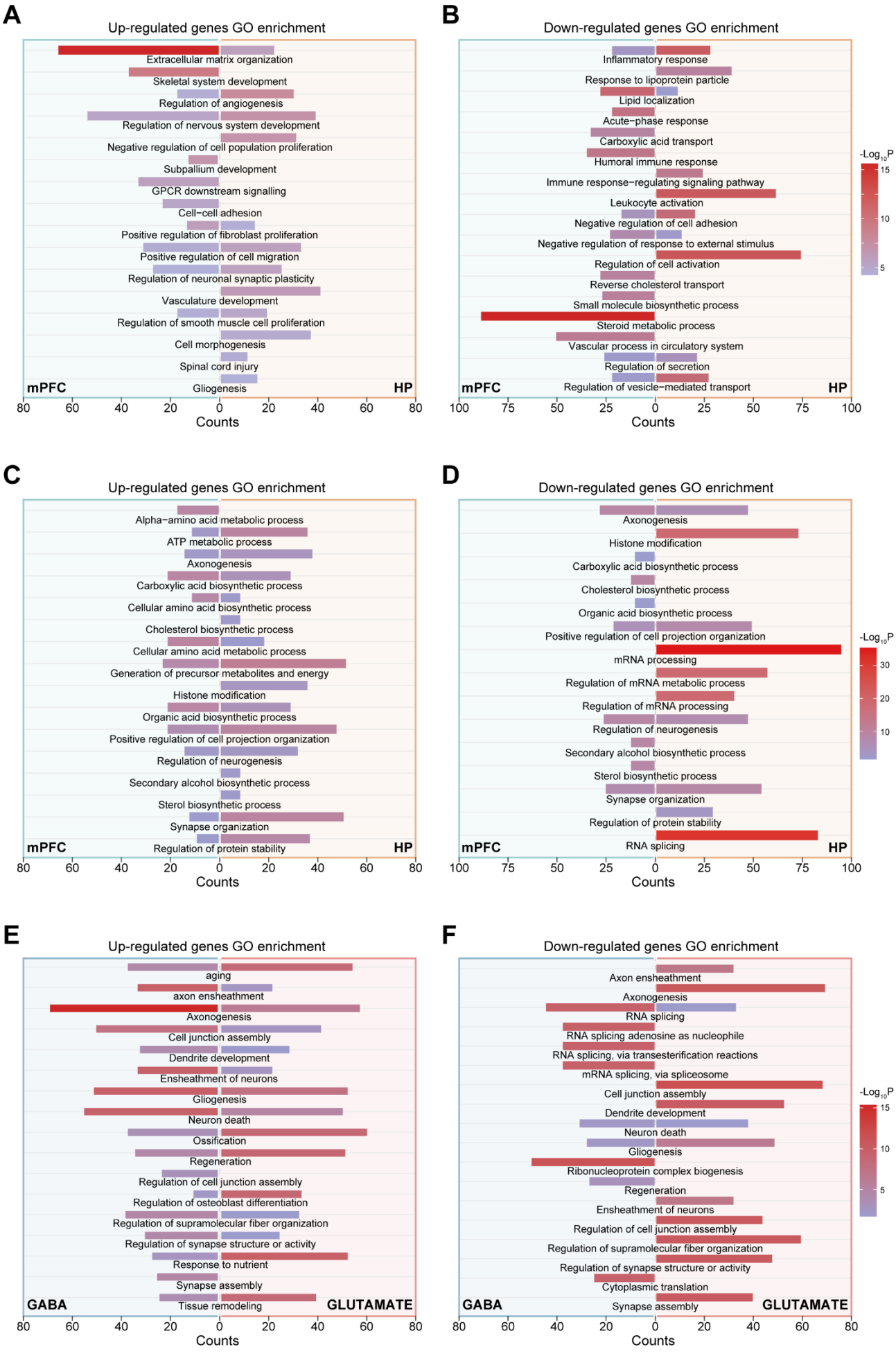
A
Up-regulated genes GO enrichment
Extracellular matrix organization
Skeletal system development
Regulation of angiogenesis
Regulation of nervous system development
Negative regulation of cell population proliferation
Subpallium development
GPCR downstream signalling
Cell−cell adhesion
Positive regulation of fibroblast proliferation
Positive regulation of cell migration
Regulation of neuronal synaptic plasticity
Vasculature development
Regulation of smooth muscle cell proliferation
Cell morphogenesis
Spinal cord injury
Gliogenesis
mPFC
HP
80 60 40 20 0 20 40 60 80
Counts
B
Down-regulated genes GO enrichment
Inflammatory response
Response to lipoprotein particle
Lipid localization
Acute−phase response
Carboxylic acid transport
Humoral immune response
Immune response−regulating signaling pathway
Leukocyte activation
Negative regulation of cell adhesion
Negative regulation of response to external stimulus
Regulation of cell activation
Reverse cholesterol transport
Small molecule biosynthetic process
Steroid metabolic process
Vascular process in circulatory system
Regulation of secretion
Regulation of vesicle−mediated transport
mPFC
HP
100 75 50 25 0 25 50 75 100
Counts
-Log10P
15
10
5
C
Up-regulated genes GO enrichment
Alpha−amino acid metabolic process
ATP metabolic process
Axonogenesis
Carboxylic acid biosynthetic process
Cellular amino acid biosynthetic process
Cholesterol biosynthetic process
Cellular amino acid metabolic process
Generation of precursor metabolites and energy
Histone modification
Organic acid biosynthetic process
Positive regulation of cell projection organization
Regulation of neurogenesis
Secondary alcohol biosynthetic process
Sterol biosynthetic process
Synapse organization
Regulation of protein stability
mPFC
HP
80 60 40 20 0 20 40 60 80
Counts
D
Down-regulated genes GO enrichment
Axonogenesis
Histone modification
Carboxylic acid biosynthetic process
Cholesterol biosynthetic process
Organic acid biosynthetic process
Positive regulation of cell projection organization
mRNA processing
Regulation of mRNA metabolic process
Regulation of mRNA processing
Regulation of neurogenesis
Secondary alcohol biosynthetic process
Sterol biosynthetic process
Synapse organization
Regulation of protein stability
RNA splicing
mPFC
HP
100 75 50 25 0 25 50 75 100
Counts
-Log10P
30
20
10
E
Up-regulated genes GO enrichment
aging
axon ensheathment
Axonogenesis
Cell junction assembly
Dendrite development
Ensheathment of neurons
Gliogenesis
Neuron death
Ossification
Regeneration
Regulation of cell junction assembly
Regulation of osteoblast differentiation
Regulation of supramolecular fiber organization
Regulation of synapse structure or activity
Response to nutrient
Synapse assembly
Tissue remodeling
GABA
GLUTAMATE
80 60 40 20 0 20 40 60 80
Counts
F
Down-regulated genes GO enrichment
Axon ensheathment
Axonogenesis
RNA splicing
RNA splicing adenosine as nucleophile
RNA splicing, via transesterification reactions
mRNA splicing, via spliceosome
Cell junction assembly
Dendrite development
Neuron death
Gliogenesis
Ribonucleoprotein complex biogenesis
Regeneration
Ensheathment of neurons
Regulation of cell junction assembly
Regulation of supramolecular fiber organization
Regulation of synapse structure or activity
Cytoplasmic translation
Synapse assembly
GABA
GLUTAMATE
80 60 40 20 0 20 40 60 80
Counts
-Log10P
15
10
5

Supplementary Figure 6. BAF155 regulates heterogeneous responses of OPCs to neuronal inputs in different brain regions

(A, B) GO analysis of the up/down-regulated genes in isolated OPCs from the mPFC and hippocampus of *Pdgfrα*^{CreER}*;Baf155*$^{fl/fl}$ mice.

(C, D) GO analysis of the up/down-regulated genes in isolated OPCs from the mPFC and hippocampus in response to GABA.

(E, F) GO analysis of the up/down-regulated genes in isolated OPCs from the mPFC in response to excitatory neurotransmitter glutamate and inhibitory neurotransmitter GABA.